

SLAG/METAL INTERACTIONS DURING FURNACE TAPPING OPERATIONS

Authors: N.W. Jones^{*}, K.G. Bain^{*}, G.J. Hassall^{*} and C.J Treadgold^{*}.

^{*} Teesside Technology Centre, Corus UK Ltd.

ABSTRACT

A Computational Fluid Dynamics (CFD) code has been combined with a computational thermodynamic model for the determination of chemical phase equilibrium, to provide a transient description of the steel/slag system during a ladle filling and alloying process. Details of the model philosophy, the basic construction of the model and assumptions are given. The results of validation of the model as applied to a production heat of high carbon silicon/manganese deoxidised steel are presented and the sensitivity of the model to process parameters such as steel oxygen content, tap slag carryover and retained slag or ladle glaze is examined.

Introduction

The continuing emphasis placed by the steelmaking community on the importance of enhancing the consistency and quality of steel has highlighted the requirement for a more complete understanding of the parameters influencing the behaviour of non-metallic inclusions during the through processing of steel. If it is accepted that the behaviour of inclusions, viz; their formation, modification and removal, is subject to, and therefore controlled by the thermodynamic and fluid dynamic conditions that the inclusions experience within the ladle as the steel is processed, then it is important that these conditions be defined. Since a dynamic system does not easily lend itself to examination by experimental means, the approach taken by a number of investigators has been to study the slag/steel system through the development of computational/mathematical models.

As reviewed previously⁽¹⁾, the development of predictive thermodynamic models to examine the equilibrium between steel and metallurgical slag has resulted in the availability of a number of commercial packages and whilst a significant degree of success in predicting the actual inclusion compositions has been achieved, it has been indicated⁽²⁾ that the application of thermodynamic modelling alone is not sufficient to predict the full range of inclusion species found in the product.

Computational modelling of fluid flow within metallurgical process operations has similarly been a subject of sustained investigation and development. In recent years commercial software packages have been extensively applied to examine slag/steel/gas mixing and fluid flow phenomena in a variety of steel processing operations. An excellent discussion on the subject of applying computational fluid dynamics to ladle steel making processes is given by Jonsson⁽³⁾. The same author has successfully incorporated chemical equilibrium routines within a fluid dynamics framework to model the behaviour of sulphur during ladle refining⁽⁴⁾.

This approach of linking fluid flow to chemical equilibrium to describe the global chemical equilibrium between phases as a combination of local equilibrium conditions is a philosophy which has been previously successfully applied to the zinc galvanising process⁽⁵⁾. Further areas of application include the RH-degassing process and vessel tapping and alloying⁽¹⁾, development of the latter being the subject of this paper which will discuss the validity of the fully integrated model, with regard to the prediction of the global and localised phase equilibrium within the ladle, as the furnace tapping and alloying process progresses.

Model Philosophy

The objective of the model is to provide a detailed time-dependent picture of the thermodynamic stability of the various phases within the ladle during the tapping and alloying period. The assumption of a global equilibrium between the steel and the slag, be it carry-over BOS slag or slaggy material coating the ladle refractories, defined by Siebring and Franken⁽⁶⁾ as ladle glaze, would impose limitations on the model's potential versatility as local equilibrium conditions would almost certainly predominate. Equally, a simple global kinetic model would be complicated to apply as the significant variations in the reaction rate equations, needed to compensate for the localised changes in fluid flow and mass transfer conditions, would influence the integrity of the predictions. Hence, the current model philosophy is to describe the internal ladle volume as a matrix of discrete cells, each of which contain the iron and dissolved species, and which, at any given point in time, can be assumed to be in chemical

equilibrium. This has been achieved by combining the computational fluid dynamics (CFD) software package (CFX) with the thermodynamic package (ChemApp).

The mass transport of species between the matrix cells within the system is dictated by the fluid flow as determined by the CFD calculations and the subsequent thermodynamic and chemical stability of phases at any position within the ladle is governed by the local equilibrium within each cell. Figure 1 gives a schematic representation of the process model concept. The modules flotation, nucleation and slag/refractory interaction are not incorporated in the existing version of the model.

Description of Model

Although the concept is for a generalised model, the basic development has been carried out on a specific production heat. The following assumptions were made concerning the construction of the model:

- (i) The ladle is symmetrical about the centre line and hence can be described by a half-ladle two dimensional geometry comprised of a mesh of 400 cells.
- (ii) The system is a single phase, of liquid iron with C, Si, Mn, O, Al, SiO_2 , Al_2O_3 , MnO, FeO, CaO and MgO as dissolved species. The top slag and ladle glaze are not integral to the fluid dynamics code.
- (iii) Alloys added to the ladle, carbon, ferromanganese, and ferro-silicon, gradually dissolve in the steel bath. The position of the alloys in the ladle is relative to their density with respect to the liquid steel.
- (iv) The temperature distribution within the ladle is determined by the enthalpy balance as governed by the boundary conditions, viz: Tapping temperature (remains constant) and heat losses from the side wall, base and slag. The chill effect of the alloy additions on the enthalpy is considered.
- (v) The oxidation of carbon is a function of the localised ferrostatic pressure and temperature, any gas formed does not react further and leaves the steel/slag system.
- (vi) Liquid or solid oxide phases formed by chemical equilibrium in the interior of the matrix remain in the steel as dissolved species. Those formed in the cells adjacent to the ladle wall or base are removed from the system to the ladle glaze. Liquid oxides formed in the cells adjacent to the slag are removed to the slag.
- (vii) As the level of steel in the ladle rises the liquid portion of oxide species in the ladle glaze is assumed to be removed to the slag which has uniform coverage and homogeneous composition at all times.

The model has currently been dimensioned to simulate the filling of a steel making ladle with a metal tap weight of 274 tonnes. Centre line symmetry of the ladle has been assumed and hence for modelling purposes is represented as a half ladle containing 400 cells, 20 each on the x and y directions and one cell deep (z direction). In order to allow the ladle to be filled in line with the run out time during tap, an expanding grid technique has been adopted; unfortunately this cannot be used to represent the ladle tap with no metal in the ladle, since this would require a

grid of zero volume. Therefore, for the period of tapping prior to the start of additions (i.e. 140 seconds), the ladle is assumed to be one third full and the grid does not expand. During this initial period (i.e. prior to grid expansion), a body force is imposed on the metal simulating the initial BOS tapping stream developing the fluid flow and allowing mass transfer of the dissolved species through the matrix. The thermodynamic calculations simulating interactions between the dissolved species (i.e. the BOS metal composition) and ladle glaze are performed from zero time, thus minimising any potential errors due to the computational technique. From 140 seconds to the end of tap at 420 seconds (7 mins; the run out time of the plant trial), the grid expands according to the tapping rate, whilst maintaining the same cell configuration.

The tapping stream enters at the top of the grid in the first two cells furthest from the side wall, thus representing a central tapping stream in a fully dimensioned ladle. During this period, the various ladle additions (e.g., C, FeMn and FeSi) are added to the appropriate matrix cells in the same sequence and rate as those in the plant trial. To allow for the density difference of the alloy additions made during tapping, these additions are modelled by directly introducing them into defined areas of the ladle. Thus, carbon and ferro-silicon are added into the grid near the top of the ladle and ferro-manganese, near to the base. At present a mathematical algorithm, 'gamma function', is used to represent the dissolution process, releasing the alloying species as a function of time, into the designated cells within the grid.

The derived top slag, any retained slag and ladle glaze associated with the side wall and base of the ladle, are held in a data array and may be visualised as a hypothetical halo of cells surrounding the exterior top, side wall and base of the grid.

The continually evolving thermodynamic equilibrium existing within the system is established by calculating, at specific time intervals, the equilibrium distribution of phases within the cells via the ChemApp software package. Three groups of calculation are considered. Every ten seconds the equilibrium between the oxide phase contained within the dummy halo of cells and the steel (and oxide if any present) in the edge cells at the top, side wall, and base of the grid is calculated. From the result of the equilibrium calculation for each 'pair' of cells, any oxide phases formed are placed in the glaze array and the steel composition fed back to the grid cell. At a thirty second interval, the equilibrium conditions existing in each of the 400 grid cells is established and the result, both oxide and steel species, from each respective cell is written back to the grid. The most frequent use of ChemApp, is at each time step, currently set to 1 second, where an equilibrium calculation on each dummy cell in the glaze array, for the side wall and base of the ladle determines the distribution of slag (liquid oxides) and any precipitated stoichiometric solid oxide compounds formed. In this case the solid oxide formed is returned to the respective area and dummy cell of the glaze array, and the sum of the liquid portion in the cells is equally distributed to the dummy cells in the top slag array to form a homogeneous top slag composition of uniform coverage.

Model Validation

A two stage approach towards validation of the model has been adopted. The initial step involved validation of the flow profile and temperature distribution as determined by the CFX code against a 1:5 scale physical water model of a filling ladle. Subsequently, once the completed user routines such as those involving determination of chemical equilibrium (as derived from the ChemApp package) and dissolution of the alloying elements had been

integrated into the code, the model was established to simulate the tapping cycle of a trial monitored production cast.

Fluid Flow Validation

To simulate the tapping of the ladle, the physical model was filled one-third full of water at 50 °C, and cold water at 17 °C was added via a perspex tube, ending just below the initial water level to prevent air entrainment. The variation in temperature of the reservoir of water was recorded by three chrome-alumel thermocouples positioned near the base of the model and the fluid flow pattern was viewed using the dispersion of neutral density polystyrene spheres. A CFD representation of the water model was constructed in CFX. Figures 2(a) and (b) respectively detail the comparison between the physical and computer generated flow profiles. Although the geometry represented in Figure 2(b) consists of a three dimensional expanding mesh (40 x 20 x 3) cells a two dimensional grid of (20 x 20 x 1) cells was found not to inhibit the accuracy of the CFX solution, whilst providing a significant reduction in computing time. Figure 3 shows the recorded temperature profiles from the thermocouples along with those predicted by CFX. The above Figures clearly illustrate the computed and measured flow and temperature profiles to be in good agreement. The results of the validation exercise indicated that a time step of 1 second each with 100 iterations was sufficient to provide convergence of the flow solution and also highlighted that the renormalisation group theory (RNG) turbulence model, was the most suitable option within CFX to model a fast flowing tapping stream entering the ladle.

Validation of the Integrated Model

Validation of the integrated model has been undertaken by comparison of results from a production heat although the obvious practical difficulty in obtaining a quantitative analysis of the slag/metal phases in the ladle during the tapping operation of the steelmaking vessel prevents a dynamic comparison between the predicted and actual phase equilibrium.

Fluid Flow

Figure 4 shows the predicted fluid flow velocity field, depicted as two half ladles, at 8 minutes and 10 minutes. At one minute after the end of tap the model indicates that the momentum of the tapping stream is still sufficiently established to maintain a flow pattern involving material driven centrally down the ladle, although at the top periphery of the ladle a small vortex has been established with a reverse flow pattern. After a further two minutes the flow direction has completely reversed, and is now dictated by the thermal distribution in the ladle, the cooler denser material adjacent to the ladle wall is displaced by material from the centre of the ladle. The average temperature of the bulk steel predicted by the model is 1566 °C, which compares well to the production sample taken following completion of tap of 1561 °C.

Ladle Chemistry

Figure 5 shows the development of the top slag on the ladle as the tapping cycle progresses. As expected, there is an initial build-up in the iron and manganese oxide content of the slag as the oxygen-rich steel equilibrates with the 'ladle glaze' coating the refractories. This continues until the first alloy additions of carbon and manganese are made which results in a significant reduction in the iron oxide content of the slag, and a further increase in manganese oxide. The subsequent introduction of silicon to the ladle rapidly reduces the iron and manganese oxide

content of the ladle, and coincides with an increase in acidity of the slag which promotes the removal of magnesia from the ladle walls. Figure 6 details the change in the total weight of slag with time. From 140 s to 420 s the weight of top slag is continuously increasing as the rise in steel level introduces new glaze to the system from the side wall. The rate of increase in slag mass with time is largely steady over this period, although it is noticeably accelerated when the silicon additions are made to the ladle. The model predicts a final slag mass of approximately 0.8 tonnes.

The introduction and dissolution of the alloy elements in the ladle results in significant concentration gradients in the system. Figure 7 illustrates the distribution of silicon in the ladle at the end of tap, (7 min) and after a further three minutes standing time. At 7 minutes the concentration profile is reflective of the fluid flow pattern as described on the left hand side of Figure 4. By the end of the simulation, at ten minutes, the silicon concentration is predicted to be uniform throughout the ladle.

The final analysed slag and metal concentrations in the ladle are compared to those predicted from the model in Table 1. Also contained in the table is the slag analysis at the start of the Ladle Arc Furnace (LAF) treatment. This is comparable to the predicted slag composition, readjusted to account for a one tonne addition of wollastonite. The predicted and measured steel silicon analysis show good agreement. For carbon and manganese however the predicted concentrations in the steel are slightly greater than measured and the slag compositions at the end of tap do not show particularly good agreement. However, following fluxing of a tonne of wollastonite with the ladle slag, the results are more comparable. Barring any significant physical yield loss of carbon and manganese additions to the ladle or alternatively errors in the slag/steel analysis, the lower apparent yield of manganese and carbon in the steel and the greater retention of manganese and iron oxide in the slag, as indicated by the actual slag/steel analysis compared to the model, suggests that possibly the ladle is more oxygen rich than predicted and/or only a fraction of the top slag is in equilibrium with the steel. If this latter statement is correct, then this implies that the interfacial kinetics of the chemical reactions at the slag/metal interface or diffusion in the slag are the predominant factors in establishing the bulk slag/steel equilibrium.

The simulation also describes the transient formation of phases within the bulk steel. Figure 8(a) to (c) shows contour levels (as normal convention, blue to red increasing with concentration) indicating the presence of gas, solid and slag phases in the ladle at various times during the filling of the ladle. The model predicts the formation of carbon monoxide gas predominately in the higher regions of the ladle and close to the oxygen rich tapping stream. A small amount of solid oxide (alumina or mullite), parts per million level, is stable again close to the tapping stream in the middle of the ladle. The formation of slag is concentrated close to the tapping stream at the base of the ladle.

Influence of Tap Oxygen and Suppression of CO evolution

It is accepted that during tapping, air entrainment at the point of impact between the metal stream and the ladle can occur leading to both nitrogen and oxygen pick-up by the steel. Yet no adequate description, suitable for incorporation into the model is known to the authors. Of equal importance to the process is the ability for carbon monoxide gas to nucleate. It can easily be demonstrated that, for homogeneous nucleation, very high over-pressures are required to nucleate a gas phase in this situation, however these over-pressures can be lowered

significantly in regions where nucleation sites already exist (heterogeneous nucleation) i.e. at ladle walls and slag/metal interfaces. In order to examine the significance of these phenomena to the ladle filling process the model was run under conditions of increasing oxygen in the tapping stream. Further simulations were carried out where, to represent suppression of the carbon monoxide evolution reaction, an over-pressure of 10 atmospheres was imposed on the equilibrium calculations in the bulk steel. For the cells adjacent to the ladle wall and base the over-pressure was set to 3 atmospheres, the assumption being a lower required nucleation energy in these areas. The results of the final predicted steel and slag analyses are given in Table 2 and indicate a shift to a more acid, higher silica containing final slag, although even the addition of a tap steel composition of 1500 ppm oxygen, in conjunction with suppressed gas evolution, is still slightly more basic than the reported post stir slag analysis. The influence of the lower slag basicity is manifested in the reduced predicted quantity of magnesia remaining on the ladle side wall at the end of tap.

The 'ladle glaze' is supersaturated in magnesia originating from the ladle refractories, the assimilation of which in a liquid oxide phase is dependant upon its combination with acidic oxides such as silica. As carbon is oxidised high in the ladle close to the tapping stream, this depletes the oxygen in the steel in this region. Silicon which is added to cells close to the top of the ladle is swept down the centre of the ladle, Figure 7, and combines, along with manganese and oxygen, deep in the bath to form a liquid slag phase. This slaggy material should in turn, when adjacent to the wall, absorb magnesia and be removed to the top slag.

Figure 9 shows the coverage of magnesia remaining on the ladle wall three minutes after the end of tap. The amount of magnesia decreases with increasing tap oxygen content and further still when the carbon monoxide evolution is suppressed. The surface coverage of magnesia on the ladle wall increases towards the top of the ladle. In all of the simulations complete removal of 'glaze' on the base of the ladle was achieved. Hence, these observations when considered along with the steel flow profile support the mechanism outlined above for the removal of 'glaze' from the ladle walls.

Suppressing the evolution of carbon monoxide in the bulk steel consequently influenced the transient formation of slag in the ladle which, compared to the base case scenario (Figure 8), moved to the top of the ladle close to the tapping stream. Figures 10 (a) and (b) show the contour levels for gas and slag respectively under the conditions of 10 atmosphere over-pressure. The formation of solid oxide was most probably eliminated due to the equilibrium favouring the presence of a liquid slag phase.

Retained Slag and B.O.S Slag Carryover

The sensitivity of the model to the effect on the ladle chemistry and slag development during tapping was examined as a function of two other process variables, namely steelmaking carryover slag and the assimilation in the slag/steel system of retained slag in the ladle from a previous cast. The nominal slag oxide compositions chosen to represent these two situations are given in Table 3. Simulations were carried out to represent 0.25, 0.5 and 1.0 tonne additions of the oxide phases. The steelmaking carryover slag was introduced to the ladle via the tapping stream and the retained slag via the 'glaze' array on the base of the ladle. Table 4 shows the final predicted steel and slag analyses, the latter incorporating a one tonne addition of wollastonite; included for comparison is the model result for the base case scenario. Whilst the final slag compositions for the simulations with the additional slag material are slightly

more basic (essentially due to the increased addition of lime to the ladle) there is not a great difference in steel or slag composition compared to the base case. However, the dynamic profile of the slag development during tap does reflect more significantly the influence of the input of carryover or retained slag. Figure 11 details the variation of iron oxide in the slag with time. The presence of steelmaking slag carryover increases the rate and quantity of transfer of iron to the slag in the initial stages of tap. Conversely, the presence of retained slag on the base of the ladle suggests reduced slag iron levels prevail. Once the alloy additions are made to the ladle rapid reduction of iron from the slag is achieved irrespective of the existing slag composition. This information suggests that, although the occurrence of poor control of slag carryover on tap from the steelmaking vessel or lack of effective ladle management (resulting in retained ladle slag) may not directly be manifested in notable problems in achieving the bulk steel specification, there will be, from heat to heat, variations in the conditions controlling the development of the ladle slag on filling the ladle. This may influence for example the composition distribution of slag derived inclusions in the steel.

Inclusion Formation

A qualitative analysis of the potential sources of inclusions formed during the ladle filling and alloying process has been undertaken, using data from the model. Two inclusion sources are considered; firstly, primary precipitates from the direct formation or precipitation of solid oxide phases within the liquid steel or from the 'glaze' material adhering to the refractory lining and secondly, precipitates derived from slag/steel interaction on initial solidification of the steel.

Primary Precipitates

At 150s, low in the ladle beneath the tapping stream and adjacent to the base of the ladle, the spinel phase $\text{FeO} \cdot \text{Al}_2\text{O}_3$ is formed, although the model predicts minute quantities, below 1 ppm. From this time to the end of tap the only solid precipitate formed is alumina (Al_2O_3) close to the tapping stream. At 420 s, the end of tap, mullite ($3\text{Al}_2\text{O}_3 \cdot 2\text{SiO}_2$) is formed again low in the ladle in the area influenced by the tapping stream, and at similar concentrations of 1 to 2 ppm.

At various stages during the filling of the ladle, the equilibrium calculations suggest the formation of the spinel phase $\text{MgO} \cdot \text{Al}_2\text{O}_3$ on the ladle lining, although the predominant location at which the oxide is formed changes during tap. For the first 3 minutes of the simulation, $\text{MgO} \cdot \text{Al}_2\text{O}_3$ is formed in the top cells on the ladle side wall only. Between 3 and 6 minutes, the precipitate appears mid-height on the side wall which, with time, increases towards the lower wall region and at the end of this period is briefly present completely across the base of the ladle. However, coincident with the start of the silicon additions to the ladle, no precipitation of $\text{MgO} \cdot \text{Al}_2\text{O}_3$ is predicted. This continues until 8 min from the start of the simulation where the presence of the compound returns to the top side wall area.

Slag Derived Inclusions

To determine the composition of inclusions derived from the calculated top slags, the slag and steel are equilibrated at a ratio of 1:10000, i.e. 100 ppm slag, at 10 °C below the liquidus temperature of the steel. This technique is used to represent the change in composition of the inclusions during solidification on sampling. The results of the calculation are given in Table 5 for the simulations involving increased oxygen entrainment in the tapping stream. For

comparison the composition of measured inclusions for 2 casts based on samples taken post stir, are given. Both reoxidation inclusions and slag derived inclusions are represented. It is encouraging to note that, other than a lower magnesia content, the measured slag derived inclusion population is similar to those predicted from the model.

Conclusions

A computer simulation of the ladle filling and alloying operation achieved through the integration of the computational thermodynamic equilibrium application, ChemApp, within the framework of the computational fluid dynamics software, CFX, has been successful in providing dynamic information on the compositional changes in the steel/slag system.

The model has been validated on a specific grade/cast of product and demonstrated to be sensitive to significant variations in process parameters.

It is anticipated that further development of the model will enhance its accuracy and range of application. The formulation of a generic model capable of being linked to similar models developed to describe other secondary steelmaking processes, will provide a useful diagnostic tool to examine the thermochemistry of liquid steel processing and provide a means of optimising process routes for the production of clean steels.

Acknowledgements

The authors would like to thank Corus Research, Development and Technology for permission to publish this paper and gratefully acknowledge the support of the European Steel and Coal Community contract No. 7210.CC/809.

References

1. G. J. Hassall, K.G. Bain, R. W. Young, and M. S. Millman: Ironmaking and Steelmaking, Vol.25, No. 4, 1998.
2. D. Dyson: *ibid*
3. L. Jonsson: Doctoral Thesis, Dept. of Metallurgy, Royal Institute of Technology, Stockholm, April 1998.
4. L. Jonsson, D. Sichen and P. Jonsson: ISIJ International, Vol 38, No.3, 1998.
5. K.J. Evans and C. J. Treadgold: Proc. Galvanisers Assoc., Jackson (Mississippi), Vol 91, 1999.
6. R. Siebring and M. C. Franken: Proc. 3rd Int. Colloq. on 'Refractories' Aachen, 1996.

TABLE 1

COMPARISON OF MODEL AND REPORTED STEEL/SLAG ANALYSES

Final Steel Analysis							
	Stream [O] ppm	[O] ppm	[%C]	[%Mn]	[%Si]		
Calculated	610	34.83	0.824	0.702	0.231		
Measured	Post Stir	88	0.78	0.59	0.23		
	LAF 1	44	0.797	0.578	0.22		
Final Slag Analysis							
		(%MnO)	(%SiO ₂)	(%Al ₂ O ₃)	(%FeO)	(%MgO)	(%CaO)
Calculated	Post Stir	0.57	29.79	11.53	0.14	20.45	37.53
	LAF 1	0.25	42.39	6.49	0.06	8.87	41.95
Measured	Post Stir	4.6	39.7	4.1	1.1	16.6	33.3
	LAF 1	5.7	42.5	3.4	2.3	9.9	35.8

TABLE 2

**FINAL STEEL AND SLAG ANALYSES -
SIMULATED AIR ENTRAINMENT AND SUPPRESSED GAS EVOLUTION**

Final Steel Analysis								
	Over Pressure (Y/N)	Stream [O] ppm	[O] ppm	[%C]	[%Mn]	[%Si]		
Calculated	N	610	34.83	0.824	0.702	0.231		
	N	1000	40.44	0.799	0.701	0.227		
	N	1500	43.29	0.767	0.7	0.224		
	Y	610	49.51	0.854	0.714	0.225		
	Y	1000	86.87	0.834	0.712	0.221		
	Y	1500	114.5	0.804	0.709	0.217		
Measured	Post Stir		88	0.78	0.59	0.23		
	LAF 1		44	0.797	0.578	0.22		
Final Slag Analysis								
	Over Pressure (Y/N)	Stream [O] ppm	(%MnO)	(%SiO₂)	(%Al₂O₃)	(%FeO)	(%MgO)	(%CaO)
Calculated	N	610	0.25	42.39	6.49	0.06	8.87	41.95
	N	1000	0.27	42.86	6.35	0.06	8.33	42.12
	N	1500	0.32	43.02	6.24	0.07	8.76	41.58
	Y	610	0.54	43.46	6.18	0.10	8.85	40.87
	Y	1000	0.76	43.72	5.93	0.14	10.01	39.44
	Y	1500	1.07	44.34	5.82	0.18	9.15	39.44
Measured	LAF 1		5.7	42.5	3.4	2.3	9.9	35.8

TABLE 3

NOMINAL COMPOSITION OF TAP CARRYOVER SLAG AND RETAINED LADLE SLAG

wt%	(%MgO)	(%CaO)	(%MnO)	(%Fe_xO_y)	(%Al₂O₃)	(%SiO₂)
BOS Slag	3.38	45.6	4.4	31.2	1.33	13
Retained Slag	7.47	48.7	0.31	1.59	15.3	24.7

TABLE 4

FINAL STEEL AND SLAG ANALYSES

SIMULATED TAP SLAG CARRYOVER AND RETAINED LADLE SLAG

Final Steel Analysis

		wt (tonnes)	[O] ppm	[%C]	[%Mn]	[%Si]
Calculated	Retained Slag	0	34.83	0.824	0.702	0.231
		1	38.02	0.84	0.715	0.23
		0.5	37.6	0.84	0.715	0.237
		0.25	37.96	0.84	0.715	0.238
	BOS Carryover	1	24.66	0.837	0.728	0.224
		0.5	30.44	0.84	0.723	0.228
		0.25	33.04	0.842	0.719	0.231
Measured	Post Stir		88	0.78	0.59	0.23
	LAF 1		44	0.797	0.578	0.22

Final Slag Analysis

		wt (tonnes)	(%MnO)	(%SiO ₂)	(%Al ₂ O ₃)	(%FeO)	(%MgO)	(%CaO)
Calculated	Retained Slag	0	0.25	42.39	6.49	0.06	8.87	41.95
		1	0.23	37.69	9.18	0.06	7.66	45.18
		0.5	0.20	40.51	7.54	0.05	8.16	43.54
		0.25	0.19	40.75	7.40	0.05	8.07	43.53
	BOS Carryover	1	0.10	39.54	5.31	0.03	7.77	47.25
		0.5	0.15	40.56	5.47	0.05	9.37	44.40
		0.25	0.20	41.83	5.71	0.05	9.24	42.97
Measured	LAF 1		5.7	42.5	3.4	2.3	9.9	36.8

TABLE 5

COMPARISON OF PREDICTED AND MEASURED INCLUSION COMPOSITIONS

	Stream [O] ppm	(%MnO)	(%SiO ₂)	(%Al ₂ O ₃)	(%FeO)	(%MgO)	(%CaO)	Temp
Calculated Slag Derived	610	9.50	39.65	10.00	0.59	14.19	26.05	1452
	1000	11.86	40.68	9.37	0.72	12.93	24.44	1454
	1500	13.56	41.35	8.56	0.81	12.97	22.76	1456
Cast 1								
Measured	Reoxidation	42.7	48.8	1.5	-	1.3	4.5	
	Cast 2							
	Slag Derived	12.4	47.4	14.8	-	4	20.5	
	Reoxidation	31.7	49.2	8.5		1.5	7.2	

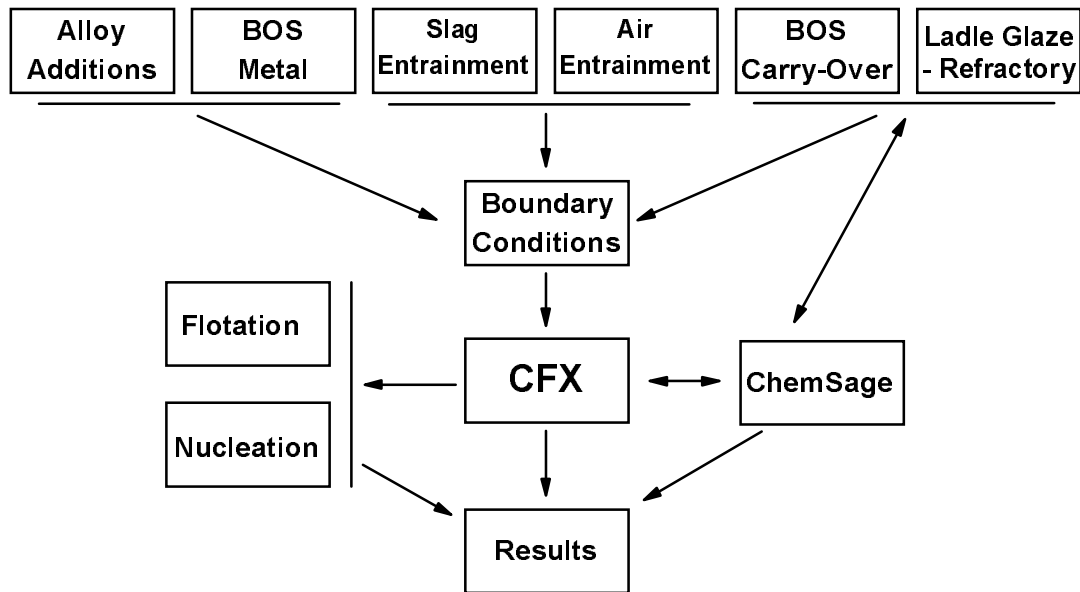


Figure 1 : Schematic Representation of the Process Model Concept

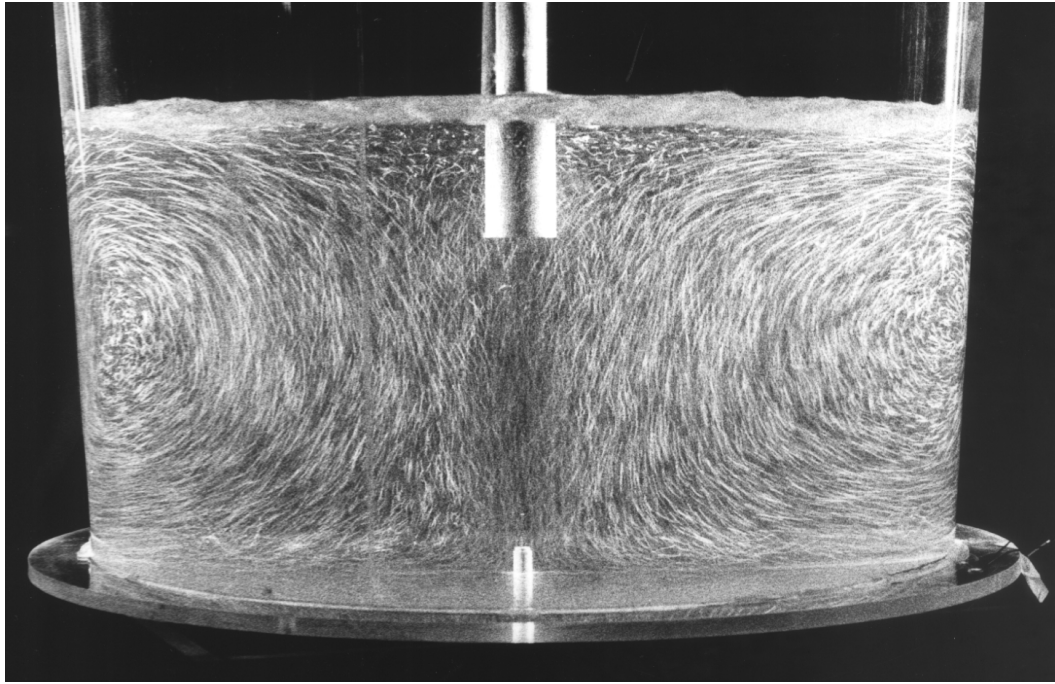


Figure 2(a) : Water Model Simulation of Filling Ladle (1/3

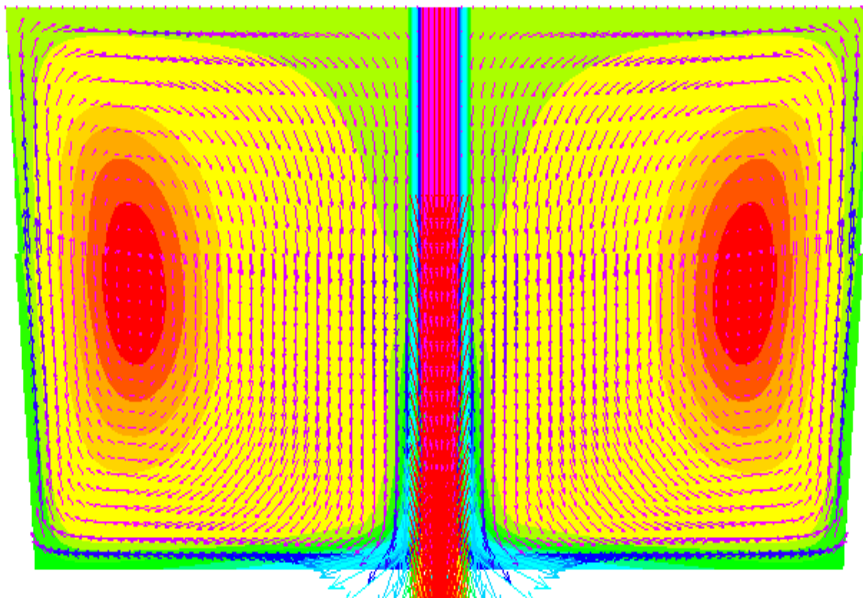


Figure 2(b) : CFX Simulation of Physical

Temperature (C)

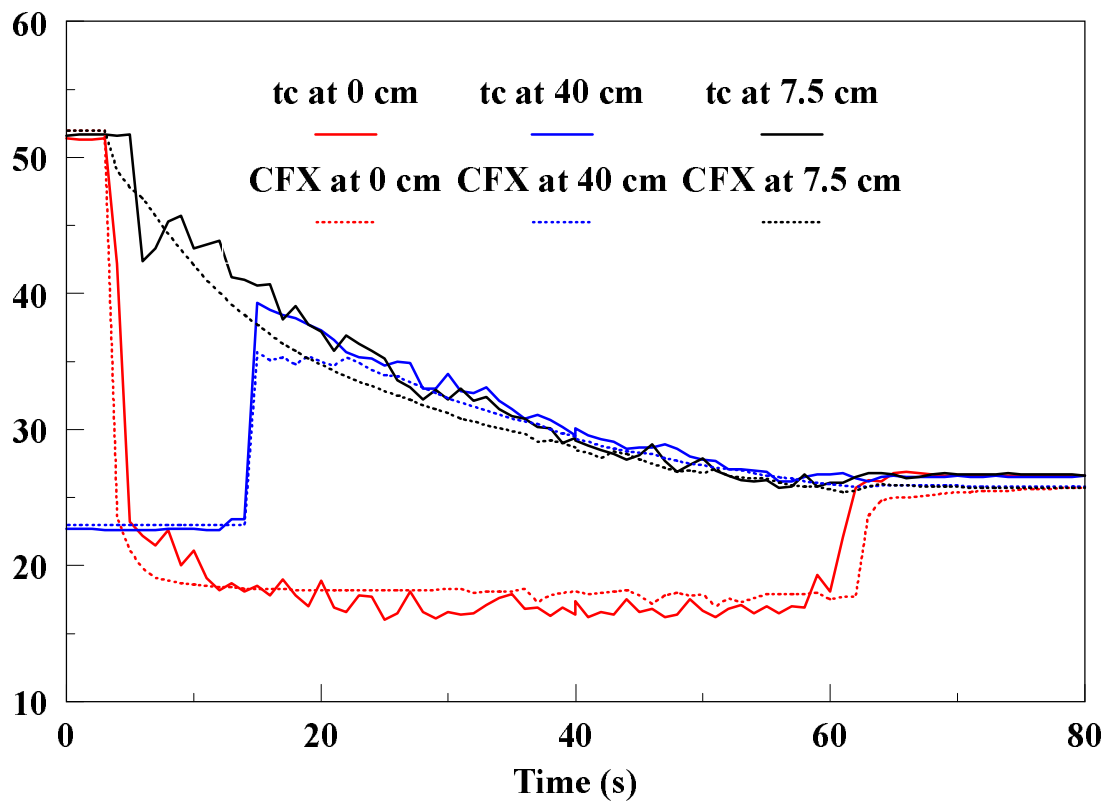


Figure 3 : Measured and Calculated Temperature Profiles (Water Model)

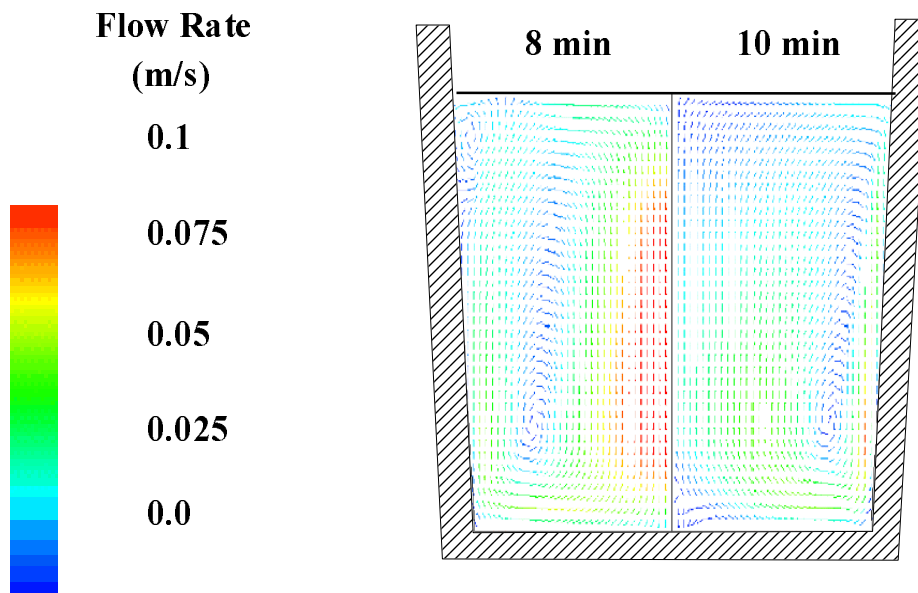


Figure 4 : Flow Pattern in Ladle at 8 & 10 minutes

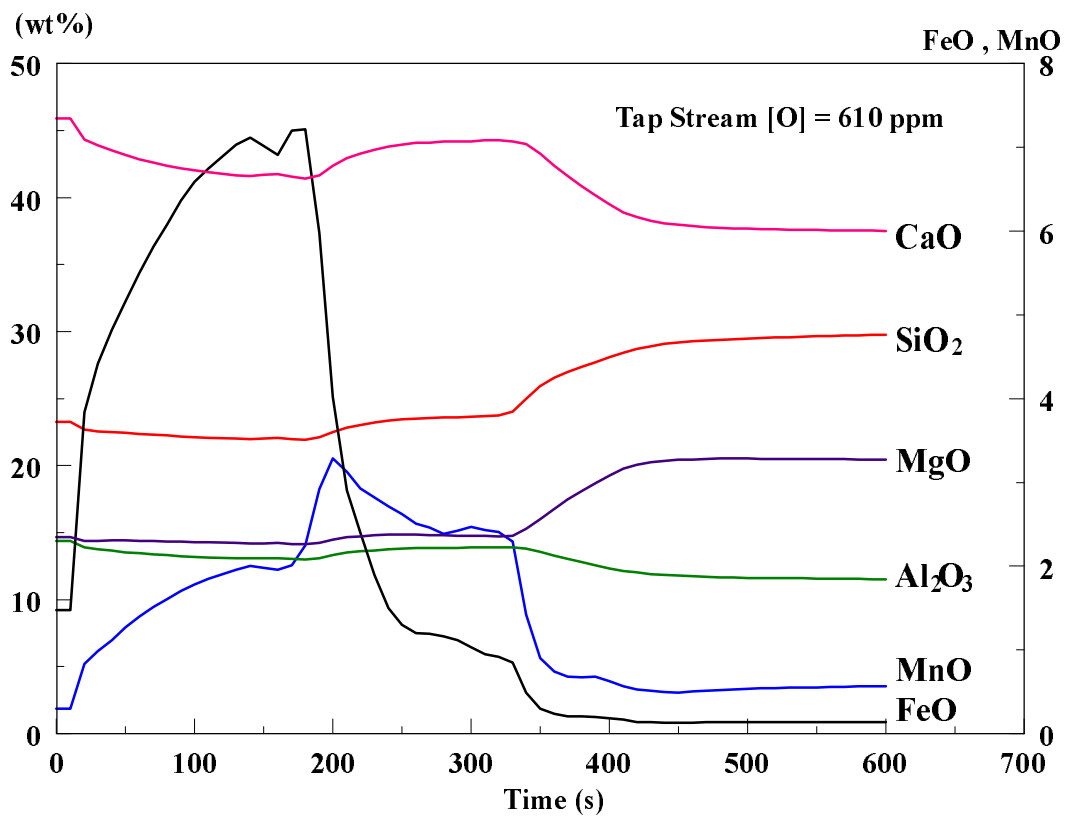


Figure 5 : Variation in Top Slag Composition With Time

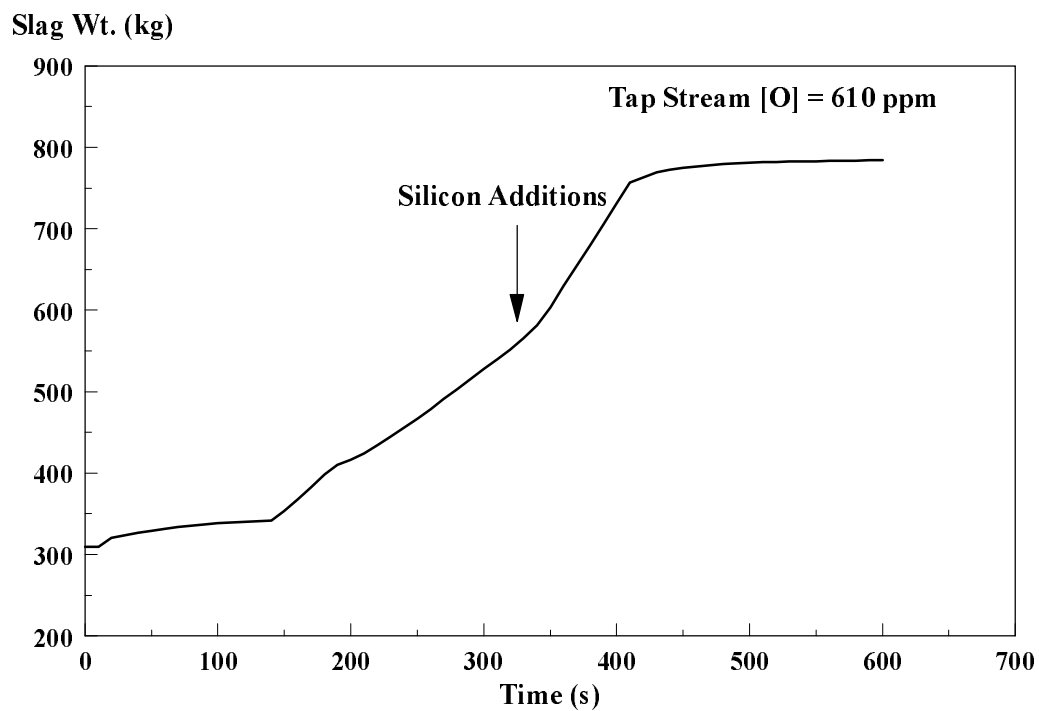


Figure 6 : Development of Mass of Top Slag During Ladle Filling

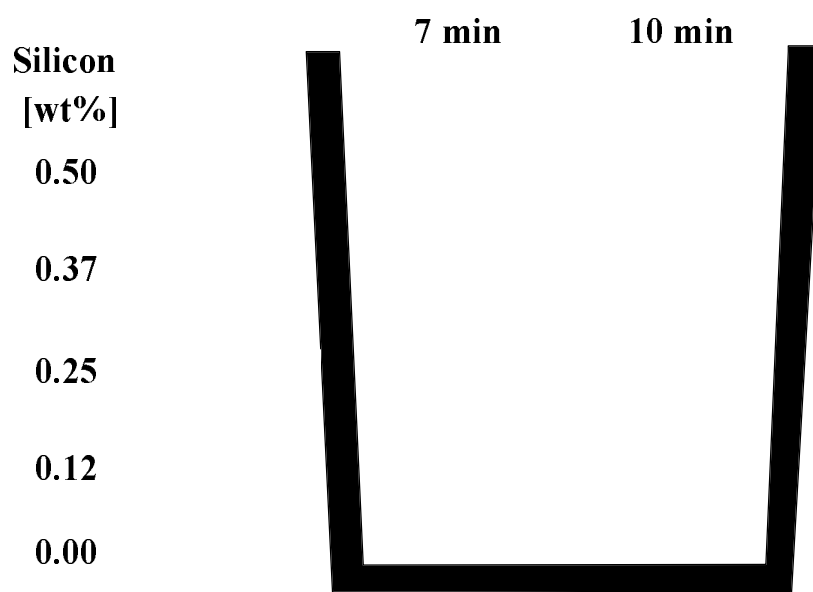
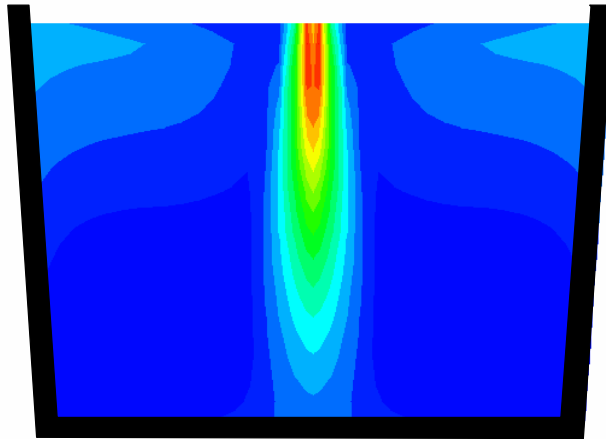


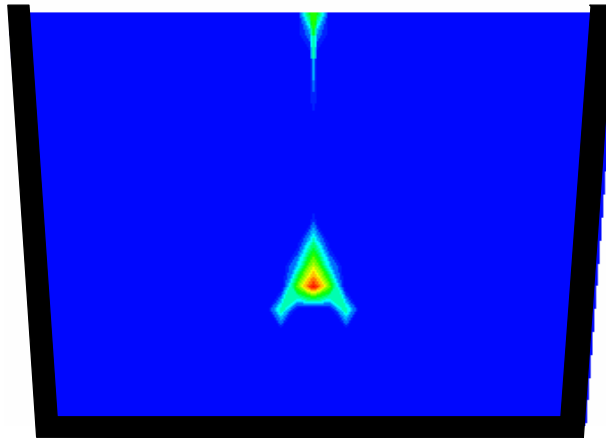
Figure 7 : Silicon Distribution at 7 & 10 minutes

Contour Plot :
Time : 5:30
Tap Oxygen : 610



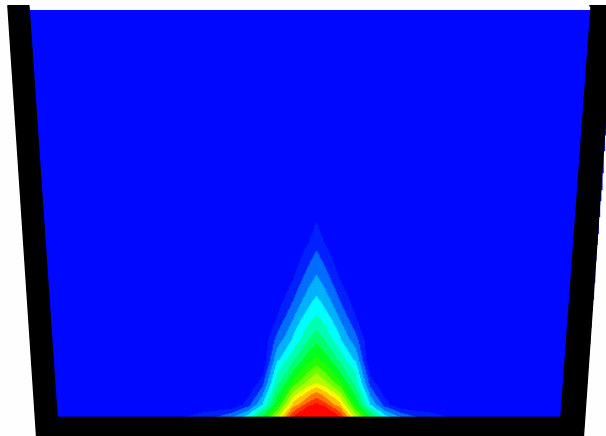
(a)

Contour Plot :
Time : 7
Tap Oxygen : 610



(b)

Contour Plot :
Time: 6:30
Tap Oxygen : 610



(c)

Figure 8 (a) to (c) : Gas,Solid & Slag Phase Formation in

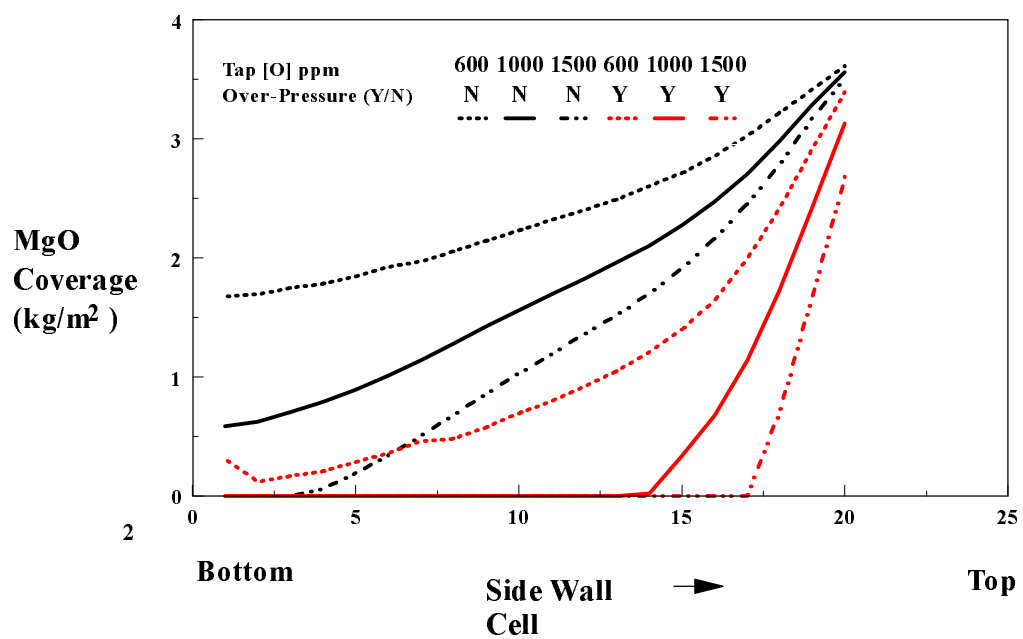
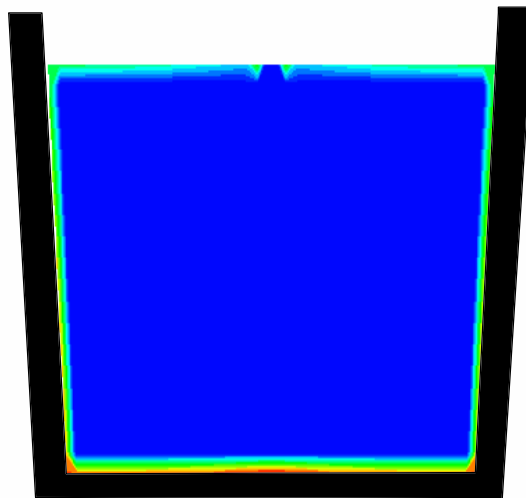


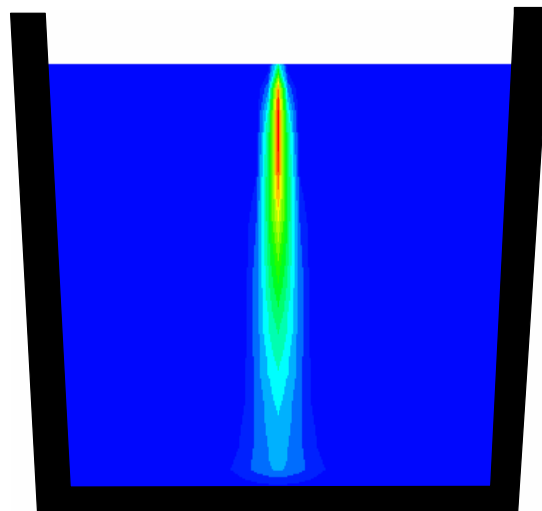
Figure 9 : Retained Magnesia on Ladle Wall at End of Tap

Contour Plot : Gas
Time : 5:30 min
Tap Oxygen : 610
Over-pressure : 10 atm



(a)

Contour Plot : Slag
Time: 6:30 min
Tap Oxygen : 610
Over-pressure : 10 atm



(b)

Figure 10 (a) & (b) : Gas & Slag Phase Formation in
10 atm Over-pressure

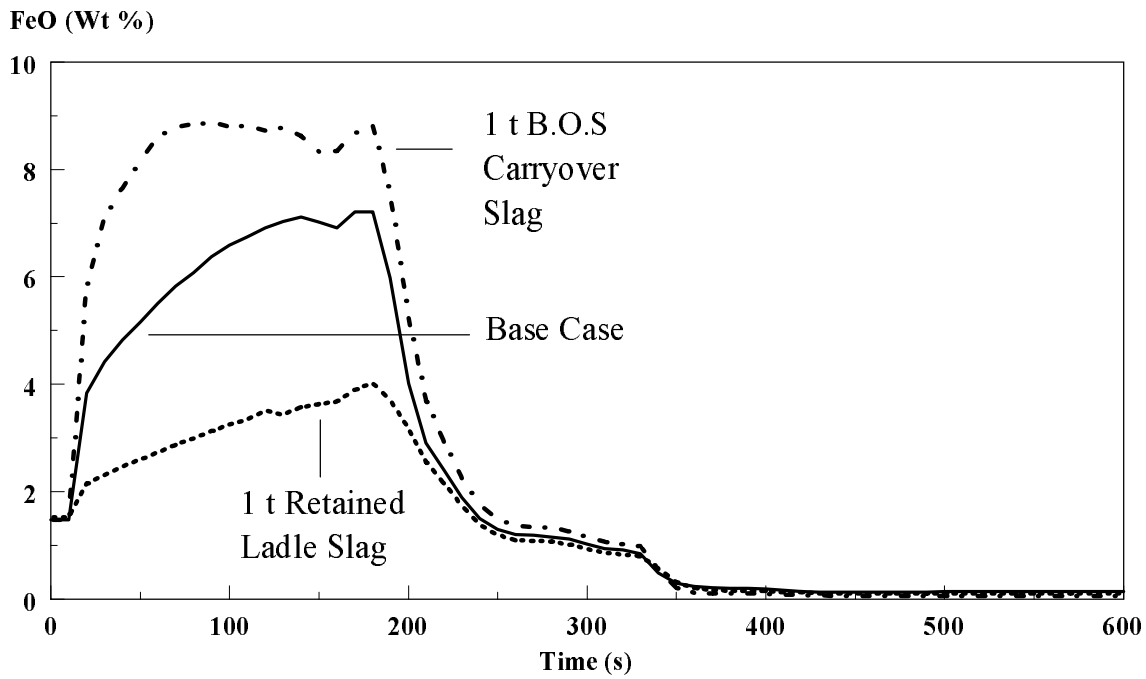


Figure 11 : Variation of FeO in Top Slag as a Function of B.O.S slag & Retained Ladle Slag Additions